

Dzyaloshinsky-Moriya interaction and the ground state in $S=3/2$ perfect kagome lattice antiferromagnet $\text{KCr}_3(\text{OH})_6(\text{SO}_4)_2$ (Cr-jarosite) studied by X-band and high-frequency ESR

Susumu Okubo^{1,2*}, Ryohei Nakata², Hitoshi Ohta^{1,2}, Shohei Ikeda², Naoki Takahashi², Takahiro Sakurai³, Wei-min Zhang², Tokuro Shimokawa^{4†}, Sakai Tôru^{5,6}, Koji Okuta⁷, Shigeo Hara^{7‡}, Hirohiko Sato⁷

¹ *Molecular Photoscience Research Center, Kobe University, 1-1 Rokkodai, Nada, Kobe, Hyogo 657-8501, Japan*

² *Graduate School for Science, Kobe University, 1-1 Rokkodai, Nada, Kobe, Hyogo 657-8501, Japan*

³ *Center for Supports to Research and Education Activities, Kobe University, 1-1 Rokkodai, Nada, Kobe, Hyogo 657-8501, Japan*

⁴ *Center for Collaborative Research and Technology Development, Kobe University, 1-1 Rokkodai, Nada, Kobe, Hyogo 657-8501, Japan* ⁵ *Japan Atomic Energy Agency, SPring-8, Sayo, Hyogo 679-5148, Japan*

⁶ *Graduate School of Material Science, University of Hyogo, Kamigori, Hyogo 678-1297, Japan*

⁷ *Department of Physics, Chuo University, Bunkyo, Tokyo 112-8551, Japan*

A single crystal $S=3/2$ perfect kagome lattice antiferromagnet $\text{KCr}_3(\text{OH})_6(\text{SO}_4)_2$ (Cr-jarosite) has been studied by X-band and high-frequency electron spin resonance (ESR). The g -values perpendicular to the kagome plane (c -axis) and in the plane are determined to be $g_c = 1.9704 \pm 0.0002$ and $g_\xi = 1.9720 \pm 0.0003$, respectively, by high-frequency ESR observed at 265 K. Antiferromagnetic resonances (AFMR) with the antiferromagnetic gap of 120 GHz are observed at 1.9 K, which is below $T_N=4.5$ K. The analysis of AFMR modes by the conventional molecular field theory shows $d_p = 0.27$ K and $d_z = 0.07$ K, where d_p and d_z are in-plane and out-of-plane components of DM d vector, respectively. From these results and the estimated exchange interaction $J=6.15$ K by Okuta *et al.*, the ground state of Cr-jarosite is discussed in connection with the Monte Carlo simulations result with classical Heisenberg spins on the kagome lattice by Elhajal *et al.* Finally, the angular dependence of linewidth and the lineshape observed at 296 K by X-band ESR show typical behavior of a two-dimensional Heisenberg antiferromagnet, suggesting a good two-dimensionality of Cr-jarosite.

1. Introduction

In condensed matter physics, frustration has been considered recently as an important and fundamental concept that plays important roles in a wide range of systems, such as magnets, metals, superconductors, multiferroics and dielectrics.¹⁾ Frustration is very interesting because it induces novel effects due to enhanced fluctuations, and frustrated systems are expected to fall into an exotic order, a new thermodynamic phase, or novel dynamics. To gain deeper insight into frustration, experiments on simple and high-quality frustrated systems are required. One candidate is a geometrically frustrated magnet. Theoretically geometrically frustrated magnets, such as triangular, kagome and pyrochlore antiferromagnets, are studied intensively.²⁾ Among two dimensional systems kagome antiferromagnet is the most interesting because it is considered theoretically to have the highest frustration, that is, the highest degree of degenerate state, and is the candidate for the spin liquid ground state.³⁾ However, even the ground state of a kagome antiferromagnet is still under debate theoretically. For instance, the presence of a gap between the ground state and the first excited state in a kagome

*sokubo@kobe-u.ac.jp

†Present address: Department of Earth and Space Science, Graduate School of Science, Osaka University, Toyonaka, Osaka 560-0043, Japan

‡Present address: Center for Supports to Research and Education Activities, Kobe University, 1-1 Rokkodai, Nada, Kobe, Hyogo 657-8501, Japan

antiferromagnet is not clearly determined among many numerical calculations.⁴⁻⁶⁾ Therefore, experiments on the model substance of kagome antiferromagnet are strongly desired, but few have been reported.⁷⁻¹⁰⁾ Moreover, the quality of kagome antiferromagnets have had some problems, such as a deficient or deformed lattice or the lack of a single crystal, as in the case, for instance, $\text{SrCr}_{9-x}\text{Ga}_{3+x}\text{O}_{19}$.^{10,11)}

Recently Okuta *et al.* succeeded in synthesizing high-quality single crystals of Cr-jarosite ($\text{KCr}_3(\text{OH})_6(\text{SO}_4)_2$) that had no defects in the Cr ions and that were large enough to allow the measurement of anisotropy in magnetization.¹²⁾ Although Cr-jarosite is expected to show magnetic properties intermediate between classical and quantum natures due to Cr ions ($S=3/2$), it is an almost ideal compound for the study of kagome lattice antiferromagnets because it shows no ion exchange or lattice distortion, which are often seen in other Cu-based or Cr-based kagome lattice model substances.^{7,8,10,11)} However, previously reported magnetic properties of Cr-jarosite were rather controversial, reflecting the difficulty in preparing good powder samples.¹³⁻¹⁶⁾ μSR and magnetization results^{13,14)} suggested a spin-glass behavior below 2 K and 4 K, respectively, while neutron diffraction results suggested a long range magnetic order with a nearly 120 degrees structure, although the transition temperature varied among reports.^{15,16)} Moreover, previous neutron studies suggested a significant deficiency of Cr atoms; that is, 76%¹⁶⁾ and 95%¹⁵⁾ Cr occupancies. On the other hand, no evidence of defects in Cr sites is obtained by the X-ray diffraction study for Cr-jarosite single crystal synthesized by Okuta *et al.*¹²⁾ The temperature dependence of magnetic susceptibility that Okuta *et al.* obtained for high-quality single crystal showed an antiferromagnetic transition accompanied by a weak ferromagnetism at $T_N=4.5$ K.¹²⁾ The frustration factor θ/T_N is estimated to be 14, suggesting strong frustration in the kagome plane of Cr-jarosite. The nearest neighbor exchange interaction J was estimated to be 6.15 K following the same analysis using a high-temperature expansion model by Morimoto *et al.*¹⁴⁾ and Harris *et al.*¹⁷⁾ Moreover, Okuta *et al.* revealed the spontaneous magnetization of $0.05 \mu_B/\text{Cr}$ along the c -axis (perpendicular to the kagome plane) below T_N ,¹²⁾ which became possible by the synthesis of single crystals. They discussed the possible origin of weak ferromagnetism as the Dzyaloshinsky-Moriya (DM) interaction and suggested that the DM vector should be perpendicular to the nearest Cr-Cr bond in the kagome plane from the consideration of the crystal symmetry.¹²⁾ However, the determination of a DM vector is rather important because the Monte Carlo simulation with classical Heisenberg spins on the kagome lattice shows that the ground state of a kagome lattice antiferromagnet depends strongly on the parameters d_p , d_z (in-plane and out-of-plane components of a DM vector), and J (the nearest neighbor exchange interaction).¹⁸⁾

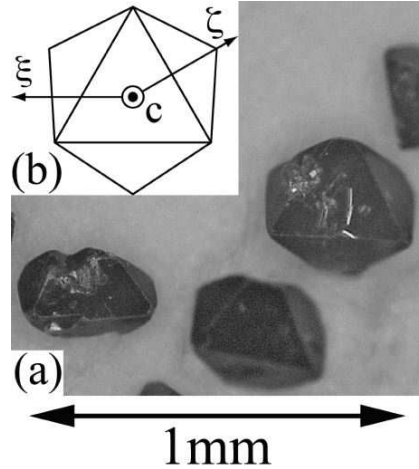


Fig. 1. (a) Photo showing the typical size of Cr-jarosite single crystals. (b) Definition of axes. The c -axis is perpendicular to the kagome plane. The ξ -axis and the ζ -axis, which are in plane with the kagome plane, are defined as the along direction and the perpendicular direction to the edge of the triangle plane of sample shape, respectively.

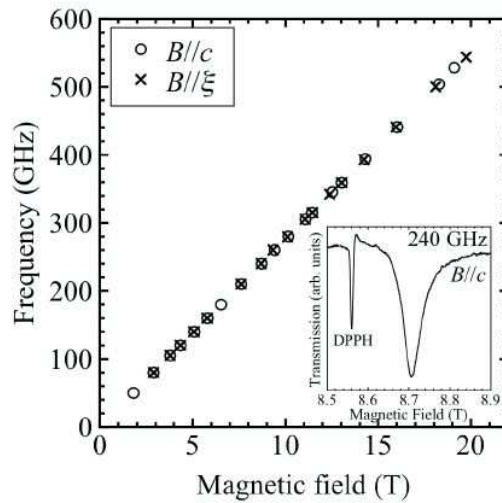


Fig. 2. Frequency-field diagram of Cr-jarosite for $B//c$ (open circles) and $B//\xi$ (crosses) observed at 265 K. The inset shows the typical ESR spectrum observed for $B//c$ at 240 GHz. DPPH is the standard of $g=2$.

On the other hand, the high-frequency high-field electron spin resonance (ESR) is a powerful means to study kagome lattice model substances^{20–22} and to determine the magnetic anisotropies of antiferromagnets.^{23,24} Especially, there are several examples^{25–27} in which the DM interaction is precisely determined by the analyses of high-frequency high-field ESR results. The aims of this study are to determine the DM interaction from high-frequency high-field ESR measurements of Cr-jarosite single crystals, and to obtain deeper insight into the ground state of Cr-jarosite.

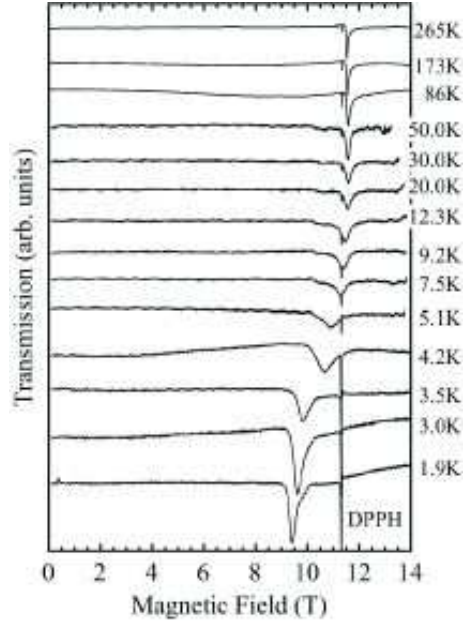


Fig. 3. Typical temperature dependence of ESR spectra observed for $B//c$ at 317.6 GHz. DPPH is the standard of $g=2$.

2. Experimental

High-frequency high-field ESR measurements of polycrystalline and single crystals of Cr-jarosite have been performed in the temperature region from 1.8 to 265 K using a pulsed magnetic field up to 16 T. Gunn oscillators and backward-traveling wave oscillators, which cover the frequency region from 80 to 481 GHz, have been used as light sources. Details of our high-frequency high-field ESR systems can be found in references.^{28–31)}

X-band (9.5 GHz) ESR measurement has also been performed using a Bruker EMX081 ESR spectrometer in the temperature region from 5 to 296 K using a He-flow cryostat. Here we should point out that the lowest temperature for X-band ESR measurement is just above the Néel temperature $T_N=4.5$ K. The angular dependence measurements have been performed by using a single crystal and a goniometer at 296 K.

Single crystals of $\text{KCr}_3(\text{OH})_6(\text{SO}_4)_2$ (Cr-jarosite) were grown by a hydrothermal method. Starting materials, $\text{K}_2\text{Cr}_2\text{O}_7$, KClO_3 , and B_2O_3 were sealed in a gold capsule with 0.3 ml of sulfuric acid (2 mol/l) solution, which was kept at 723 K under 150 MPa of hydrostatic pressure for one day. The crystal structure was analyzed using a cylindrical imaging-plate type single-crystal X-ray diffractometer. As a result of the hydrothermal reaction, we obtained dark-brown crystals shaped as deformed octahedrons. X-ray diffraction measurement revealed a hexagonal unit cell with the lattice parameters $a = 7.226 \text{ \AA}$ and $c = 17.221 \text{ \AA}$. See

Fig. 1 in ref.,¹²⁾ how kagome lattice of Cr atoms is formed.

Figure 1 (a) shows the single crystals. Typical size is about 0.4 mm. ξ and c axes are defined as shown in Fig. 1 (b). Twenty-five single crystals are aligned on a polyethylene sheet, where c -axis is perpendicular to the sheet, in order to increase the high-frequency high-field ESR intensity.

3. Results and discussion

Figure 2 shows the frequency-field diagram observed for $B//c$ and $B//\xi$ at 265 K. The inset shows the typical spectrum observed for $B//c$ at 240 GHz. As it gives relatively sharp ESR, the resonance field can be determined rather precisely. Therefore, we can obtain rather precise g -values $g_c = 1.9704 \pm 0.0002$ and $g_\xi = 1.9720 \pm 0.0003$. These values are very typical for Cr^{3+} ion in the octahedral crystal field.³²⁾ Obtained g -values are consistent with X-band ESR measurements at 294 K, the results and detailed discussion will appear in a latter section.

Figure 3 shows the typical temperature dependence observed at 317.4 GHz for $B//c$. For simplicity, some of the observed temperatures are not shown. The change in the S/N ratio between above 86 K and below 50 K is due to the change of cryostat^{28,30)} and not intrinsic. The shift in resonance starts a little higher than the Néel temperature $T_N=4.5$ K. The shift in the resonance field clearly suggests the appearance of an internal field. The divergence of linewidth, which is typical of antiferromagnetic order is also observed around T_N .

Figure 4 shows the temperature dependence of effective g -values observed at X-band (9.5 GHz), 160 GHz and 317.6 GHz for $B//c$ and $B\perp c$. Although the X-band measurement cannot reach temperatures below T_N , observed absorptions for 160 and 317.4 GHz show clear increases in g -values below T_N , suggesting the presence of an internal field. Moreover, we can also see clear divergences of linewidths at around T_N for all frequencies for $B//c$ and $B\perp c$ in Fig. 5. These results suggest that observed absorption lines below T_N are antiferromagnetic resonances (AFMR) and that the critical behavior observed around T_N is typical for the antiferromagnetic order.

Figures 6 (a) and (b) show typical AFMR observed at 1.9 K for $B//c$ and $B\perp c$. We can clearly see that main AFMR signals denoted by triangles and open circles. It is also clear that the intensities of AFMR are much stronger for $B//c$ than for $B\perp c$ in comparison with that of DPPH. The small resonances observed just below DPPH, which is the standard of $g=2$, for 130 or 160 GHz in Fig. 6 (a) seem to be the impurity resonances because their g -value are close to 2 even at the antiferromagnetic order phase. When we increased the quantity of the sample by using polycrystalline samples, we started to see weak signals denoted by solid

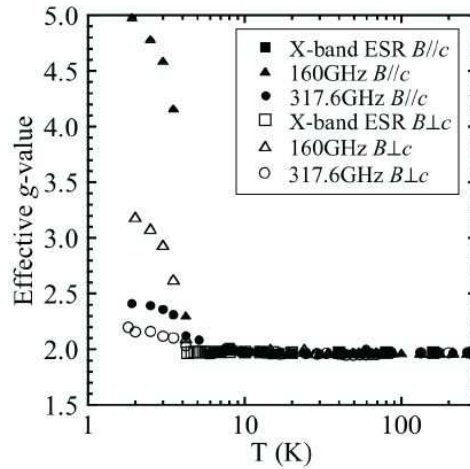


Fig. 4. Temperature dependences of effective g -value.

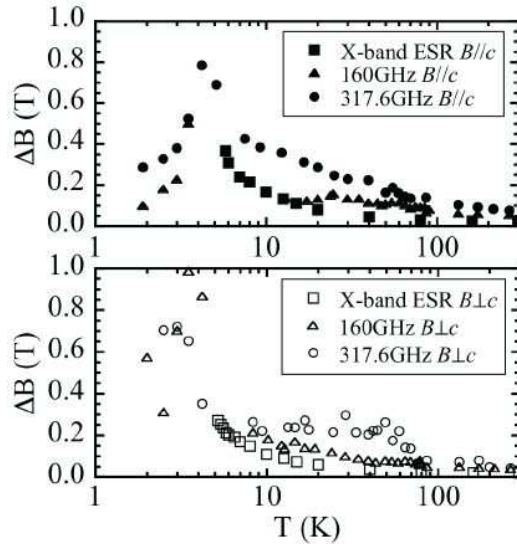


Fig. 5. Temperature dependences of linewidth.

circles as shown in Fig. 6 (c). As these signals are observed at 1.9 K and the resonance fields are far from DPPH, these weak resonances can be considered AFMR.

The AFMR's shown in Fig. 6 are plotted in the frequency-field diagram of Fig. 7. The observed antiferromagnetic gap is about 120 GHz. AFMR theory for kagome lattice antiferromagnet based on the molecular field theory is discussed by Fujita *et al.*²⁶⁾ Fujita *et al.*²⁶⁾ considered both DM model and crystal field model. However, as it turned out that it was difficult to interpret both the magnetization and AFMR results simultaneously by the crystal field model in Fe-jarosite, they discussed with the DM model. Due to the symmetry of kagome lattice, DM interaction exists,¹⁸⁾ and the DM vector d_{ij} exists in the mirror plane between the

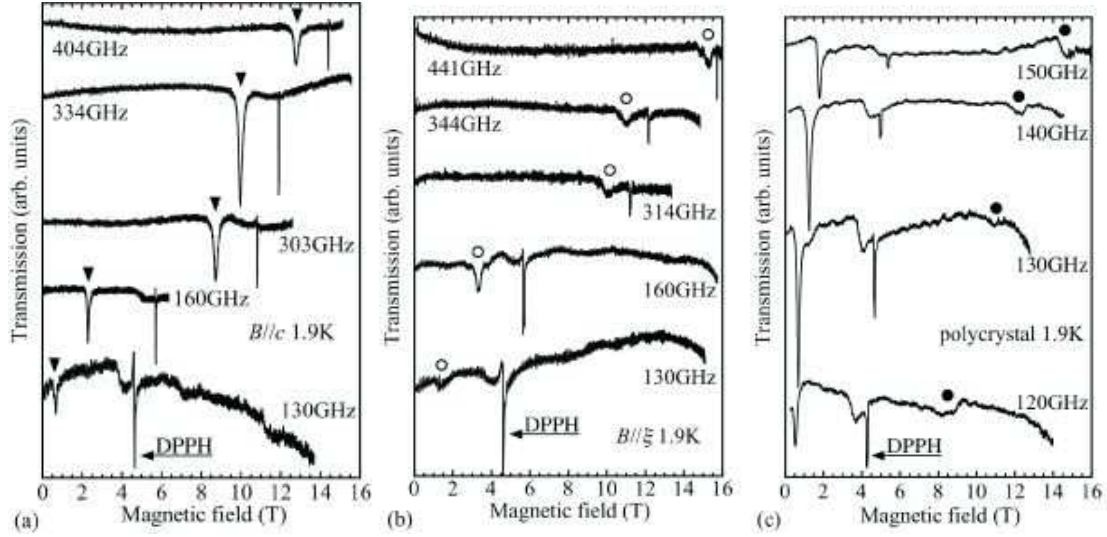


Fig. 6. Frequency dependence of AFMR spectra at 1.9 K for $B//c$ (a), $B//\xi$ (b) and polycrystal (c). DPPH is the standard of $g=2$.

nearest i and j sites in the kagome lattice following the Moriya rule.³³⁾ Fujita *et al.* considered not only the nearest neighbor exchange interaction J in the kagome plane and the DM interaction (DM vector d , see Fig. 4 in ref.²⁶⁾ for the definition of DM vector.) but also the inter plane exchange interaction J_{\perp} , and considered six sublattices in order to explain also the magnetization jump at 16.4 T observed in K-Fe jarosite. However, as no such magnetization jump is observed in Cr-jarosite,¹²⁾ we will deal with the following Hamiltonian without the inter plane exchange interaction and consider only three sublattices.

$$F = A\mathbf{M}_i \cdot \mathbf{M}_j + d_{ij} \cdot \mathbf{M}_i \times \mathbf{M}_j - \mathbf{M}_i \cdot \mathbf{B} \quad (1)$$

where $A = 6J/N(g\mu_B)^2$, $d_{ij} = 6\mathbf{d}_{ij}/N(g\mu_B)^2$, and $\mathbf{M}_i = Ng\mu_B\mathbf{S}/3$. Here N is the number of magnetic ions, and \mathbf{M}_i is the magnetic moment on the i th sublattice. Following the AFMR theory for $B//c$ described in ref. 26, we are able to interpret the observed AFMR's as shown by the solid line in Fig. 7. Here we assumed that weak AFMR's observed in Fig. 6 (c) are AFMR's for $B//c$. We used the g -value $g=1.97$, which is obtained at 265 K (Fig. 2), and $J=6.15$ K, which was obtained by Okuta *et al.* from the analysis of magnetic susceptibility.¹²⁾ The obtained parameters to interpret observed the AFMR's are $d_p = 0.27$ K and $d_z = 0.07$ K, where d_p and d_z are in-plane and out-of-plane components of the DM d vector, respectively. Order estimation of d can be made by the following equation:³³⁾

$$d_{\text{est}} = \frac{\Delta g}{g} 2J = 0.09\text{K} \quad (2)$$

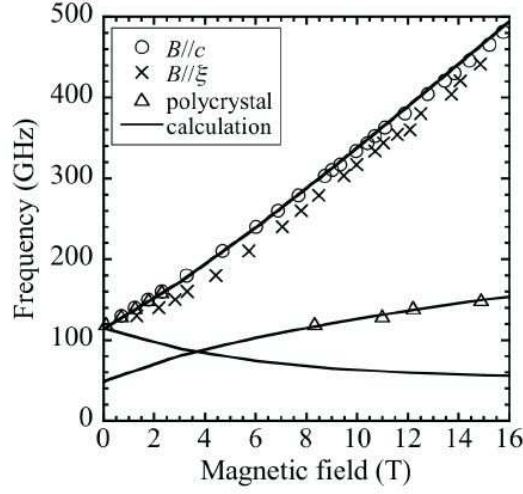


Fig. 7. Frequency-field diagram of AFMR at 1.9 K. Open circles, crosses, and open triangles correspond to $B//c$, $B//\xi$ and polycrystal, respectively. The solid lines shows the AFMR theory considering the DM interaction for $B//c$.

where Δg is obtained from the ESR result at 265 K. d_{est} is smaller than that obtained by the analysis of AFMR, but is rather acceptable for the order estimation.

The existence of DM interaction causes the spin canting, and the spontaneous magnetization is expected at low temperature. Elhajal *et al.*¹⁸⁾ suggested the canting angle η (eq. (3)) from the kagome plane to the c -axis in the kagome system with the competition between the exchange and DM interactions.

$$\tan(2\eta) = \frac{2d_p}{\sqrt{3}J + d_z} \quad (3)$$

Using the parameters $J=6.15$ K, $d_p = 0.27$ K, and $d_z = 0.07$ K, the obtained canting angle is $\eta = 1.44$ degrees. Using this angle, the expected spontaneous magnetization is calculated to be $0.074\mu_B/\text{Cr}$, which is rather comparable to the spontaneous magnetization of $0.05 \mu_B/\text{Cr}$ observed along the c -axis by Okuta *et al.*¹²⁾ Therefore, we can say that the obtained values of d_p and d_z by the analysis of AFMR are reasonable with the macroscopic measurement.

Next we discuss about the ground state of Cr-jarosite. If we compare our obtained parameters $d_z/J = 0.011$ and $d_p/J = 0.044$ versus the result of the Monte Carlo simulations with classical Heisenberg spins on the kagome lattice by Elhajal *et al.* (Fig. 5 in ref¹⁸⁾), the result clearly suggests that the ground state of Cr-jarosite corresponds to the chirality (a) shown in Fig. 8. This is rather consistent with the spontaneous magnetization along the c -axis (perpendicular to the kagome plane) observed by Okuta *et al.* below T_N ,¹²⁾ because the chirality (a) possesses a weak ferromagnetism from the result of Elhajal *et al.*¹⁸⁾ It is also consistent

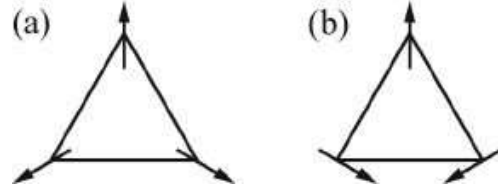


Fig. 8. Two possible chiralities (a) weak ferromagnetism perpendicular to the kagome plane and (b) coplanar structure depending on d_p and d_z discussed by Elhajal *et al.*¹⁸⁾ Our results suggest (a) for Cr-jarosite. See text for details.

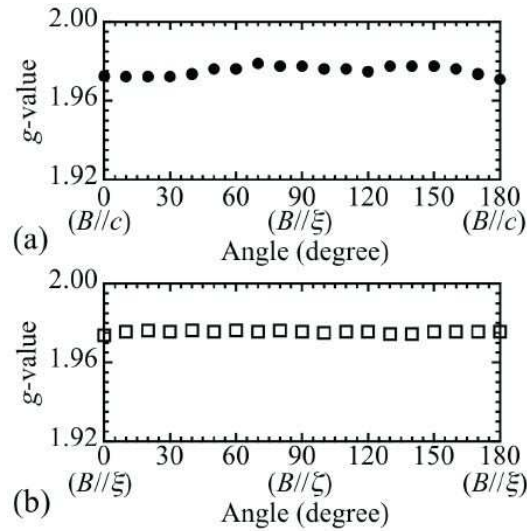


Fig. 9. Angular dependence of g -values observed at 296 K using the X-band ESR. (a) Closed circles correspond to $B//c$ (0°) to $B//\xi$ (90°) in the c - ξ plane. (b) Open squares correspond to $B//\xi$ (0°) to $B//\zeta$ (90°) in the ξ - ζ plane.

the ground state discussed for Cr-jarosite by A. S. Wills.¹⁹⁾ Moreover, the chirality (a) is also consistent with the magnetic structure suggested from the neutron result by Inami *et al.*¹⁵⁾

Finally we discuss the X-band ESR results observed at 296 K. As the linewidth of Cr-jarosite is relatively sharp, about 0.02 T, X-band ESR measurement using only a single crystal is possible and will enable us to obtain precise information about the anisotropy and the dimensionality of Cr-jarosite in the paramagnetic state. The angular dependence of g -value is very isotropic in the ξ - ζ , plane (kagome plane), while small anisotropy is observed in the c - ξ plane, as shown in Fig. 9. The obtained g -values are consistent with those obtained by high-frequency high-field ESR shown in Fig. 2. The angular dependence of linewidth is also very isotropic in the ξ - ζ plane, while a very peculiar angular dependence is observed in the c - ξ plane with the minimum at around 60° from the c -axis, as shown in Fig. 10. Figure 11

shows the line shape analysis of X-band ESR spectra observed at 296 K for $B//c$, for $B//\xi$, for 60° from $B//c$ in the c - ξ plane. They clearly show that the line shape is nearly Lorentzian for 60° from $B//c$ in the c - ξ plane (c), while other two cases are in between the Gaussian and Lorentzian.

Richards and Salamon discussed the ESR of two-dimensional Heisenberg antiferromagnet (K_2MnF_4), theoretically assuming the diffusive motion for the long-time dependence of the time correlation functions.³⁴⁾ They showed that the angular dependence of ESR linewidth had roughly the form $(3 \cos^2 \theta - 1)^2 + (\text{const.})$ (see Fig. 5 in ref.³⁴⁾ where θ is the angle of DC magnetic field with respect to the perpendicular to the two-dimensional plane), which was consistent with the experiment with K_2MnF_4 , where the linewidth is larger at $\theta = 0^\circ$ than at $\theta = 90^\circ$, with a minimum at around $\theta = 55^\circ$. This result is rather consistent with our result in the c - ξ plane with the minimum at around 60° from the c -axis as shown in Fig. 10(a). The solid line indicates best fit line of $\Delta B = \alpha(3 \cos^2 \theta - 1)^2 + \beta$ with parameters $\alpha = 21.8$ and $\beta = 175.9$. This suggested that the angular dependence of linewidth could not be explained by either the secular or nonsecular parts of the second moment, which suggests that the linewidth is larger at $\theta = 90^\circ$ than at $\theta = 0^\circ$ (see Fig. 2 in ref.³⁴⁾), which was due explicitly to the dominance of wavevector $q=0$ modes in the long-time decay of correlations in a two-dimensional system. Small discrepancy between the fit and the data in Fig. 10(a) may be coming from the DM interaction, which is not considered in ref.³⁴⁾ Moreover, they also showed that the room-temperature line shapes were Lorentzian at $\theta = 55^\circ$ and in between the Lorentzian and Gaussian at $\theta = 0^\circ$, consistent with the experiment of K_2MnF_4 . Again, this is consistent with our results in Fig. 11. From these results, we can say that Cr-jarosite is a good two-dimensional system from the standpoint of ESR at 296 K.

4. Conclusion

X-band and high-frequency ESR measurements of high-quality $S=3/2$ kagome lattice antiferromagnet $\text{KCr}_3(\text{OH})_6(\text{SO}_4)_2$ (Cr-jarosite) single crystals have been performed for the first time. Taking advantage of single crystals we are able to determine the g -values at 265 K as $g_c = 1.9704 \pm 0.0002$ and $g_\xi = 1.9720 \pm 0.0003$, whose anisotropy is very small. The temperature dependence of ESR shows the divergence of linewidth at around $T_N=4.5$ K and the existence of an internal field below T_N . AFMR modes with an antiferromagnetic gap of 120 GHz have been revealed by high-frequency ESR measurement at 1.9 K. Their analysis by the conventional molecular field theory shows $d_p=0.27$ K and $d_z=0.07$ K, where d_p and d_z

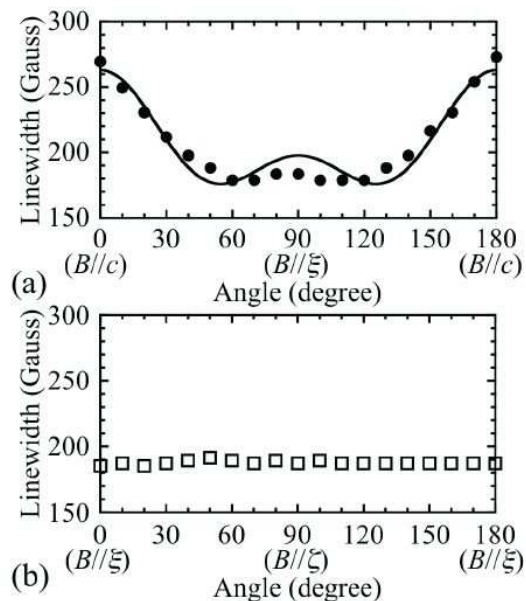


Fig. 10. Angular dependence of linewidths observed at 296 K using the X-band ESR. (a) Closed circles correspond to $B//c$ (0°) to $B//\xi$ (90°) in the c - ξ plane. The solid line is a fitting line. (b) Open squares correspond to $B//\xi$ (0°) to $B//\zeta$ (90°) in the ξ - ζ plane.

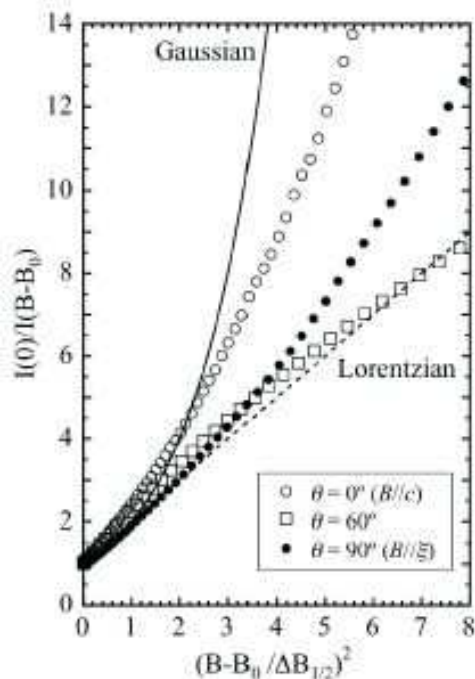


Fig. 11. Line shape analysis of ESR spectra observed at 296 K using the X-band ESR. Open circles, closed circles and open squares correspond to $\theta = 0^\circ$ ($B//c$), $\theta = 90^\circ$ ($B//\xi$), and $\theta = 60^\circ$ in the c - ξ plane, respectively.

are in-plane and out-of-plane components of DM d vector, respectively. These results are discussed in connection with the Monte Carlo simulations result with classical Heisenberg spins on the kagome lattice by Elhajal *et al.*,¹⁸⁾ and the ground state of Cr-jarosite turns out to be the chirality (a) state shown in Fig. 8 with weak ferromagnetism, which is consistent with other experimental results, including a neutron experiment. Finally, the angular dependence of linewidth and the lineshape observed at 296 K by X-band ESR turn out to be very similar to those of K_2MnF_4 , which is a typical two-dimensional antiferromagnet, and to those discussed by Richards and Salamon theoretically on two-dimensional antiferromagnets. In conclusion, we can suggest that Cr-jarosite is an ideal model substance for an $S=3/2$ Heisenberg kagome lattice antiferromagnet with good two-dimensionality from the point of view of ESR.

Acknowledgments

This work was supported by Grants-in-Aid for Scientific Research (C) No. 26400335 and No. 21550139 and for Young Scientists (B) No. 26800169 from the Japan Society for the Promotion of Science (JSPS) and by Grants-in-Aid for Scientific Research on Priority Areas No. 19052005 "Novel States of Matter Induced by Frustration" from the Ministry of Education, Culture, Sports, Science and Technology (MEXT) of Japan.

References

- 1) Special Topics Section "Novel States of Matter Induced by Frustration", J. Phys. Soc. Jpn. **79** (2010).
- 2) A. P. Ramirez, Annu. Rev. Mater. Sci. **24**, 453 (1994).
- 3) L. Balents, Nature **464**, 199 (2010).
- 4) C. Waldtmann, H.-U. Everts, B. Bernu, C. Lhuillier, P. Sindzingre, P. Lecheminant and L. Pierre, Eur. Phys. J. B **2**, 501 (1998).
- 5) P. Mendels and F. Bert, J. Phys. Soc. Jpn. **79**, 011001 (2010).
- 6) H. Nakano and T. Sakai, J. Phys. Soc. Jpn. **80**, 053704 (2011).
- 7) M. P. Shores, E. A. Nytko, B. M. Bertlett and D. G. Nocera, J. Am. Chem. Soc. **127**, 13462 (2005).
- 8) Z. Hiroi, M. Hanawa, N. Kobayashi, M. Nohara, H. Takagi, Y. Kato and M. Takigawa, J. Phys. Soc. Jpn. **70**, 3377 (2001).
- 9) Y. Okamoto, H. Yoshida and Z. Hiroi, J. Phys. Soc. Jpn. **78**, 033701 (2009).
- 10) X. Obradors, A. Labarta, A. Isalgue, J. Tejada, J. Rodriguez and M. Pernet, Solid State Commun. **65**, 189 (1988).
- 11) A. P. Ramirez, G. P. Espinosa and A. S. Cooper, Phys. Rev. **64**, 2070 (1990).
- 12) K. Okuta, S. Hara, H. Sato, Y. Narumi and K. Kindo, J. Phys. Soc. Jpn. **80**, 063703 (2011).
- 13) A. Keren, K. Kojima, L. P. Le, G. M. Luke, W. D. Wu, Y. J. Uemura, M. Takano, H. Dabkowska and M. J. P. Gingras, Phys. Rev. B **53**, 6451 (1996).
- 14) T. Morimoto, M. Nishiyama, S. Maegawa and Y. Oka, J. Phys. Soc. Jpn. **72**, 2085 (2003).
- 15) T. Inami, T. Morimoto, M. Nishiyama, S. Maegawa, Y. Oka and H. Okumura, Phys. Rev. B **64**, 054421 (2001).
- 16) S.-H. Lee, C. Broholm, M. F. Collins, L. Heller, A. P. Ramirez, Ch. Kloc, E. Bucher, R. W. Erwin and N. Lucevic, Phys. Rev. B **56**, 8091 (1997).
- 17) A. B. Harris, C. Kallin and A. J. Berlinsky, Phys. Rev. B **45**, 2899 (1992).
- 18) M. Elhajal, B. Canals and C. Lacroix, Phys. Rev. B **66**, 014422 (2002).
- 19) A. S. Wills, Can. J. Phys. **79**, 1501 (2001).
- 20) H. Ohta, M. Sumikawa, M. Motokawa, H. Kikuchi and H. Nagasawa, J. Phys. Soc. Jpn. **65**, 848 (1996).

- 21) W. Zhang, H. Ohta, S. Okubo, M. Fujisawa, T. Sakurai, Y. Okamoto, H. Yoshida and Z. Hiroi, J. Phys. Soc. Jpn. **79**, 023708 (2010).
- 22) H. Ohta, W. Zhang, S. Okubo, M. Fujisawa, T. Sakurai, Y. Okamoto, H. Yoshida and Z. Hiroi, Phys. Status Solidi B, **247**, 679 (2010).
- 23) M. Date, J. Phys. Soc. Jpn. **16**, 1337 (1961).
- 24) H. Ohta, N. Yamauchi, T. Nanba, M. Motokawa, S. Kawamata and K. Okuda, J. Phys. Soc. Jpn. **62**, 785 (1993).
- 25) S. Okubo, T. Ueda, H. Ohta, W. Zhang, T. Sakurai, N. Onishi, M. Azuma, Y. Shimakawa, H. Nakano and T. Sakai, Phys. Rev. B **86**, 140401 (2012).
- 26) T. Fujita, H. Yamaguchi, S. Kimura, T. Kashiwagi, M. Hagiwara, K. Matan, D. Grohol, D. G. Nocera and Y. S. Lee, Phys. Rev. B **85**, 094409 (2012).
- 27) M. Fujisawa, K. Shiraki, S. Okubo, H. Ohta, M. Yoshida, H. Tanaka, T. Sakai, Phys. Rev. B **80**, 012408 (2009).
- 28) M. Motokawa, H. Ohta and N. Makita, Int. J. Infrared MMW **12**, 149 (1991).
- 29) S. Kimura, H. Ohta, M. Motokawa, S. Mitsudo, W.-J. Jang, M. Hasegawa and H. Takei, Int. J. Infrared MMW **17**, 883 (1996).
- 30) N. Nakagawa, T. Yamada, K. Akioka, S. Okubo, S. Kimura and H. Ohta, Int. J. Infrared MMW **19**, 167 (1998).
- 31) H. Ohta, M. Tomoo, S. Okubo, T. Sakurai, M. Fujisawa, T. Tomita, M. Kimata, T. Yamamoto, M. Kawauchi and K. Kindo, J. Phys.: Conf. Series **51**, 611 (2006).
- 32) Electron Paramagnetic Resonance of Transition Ions, A. Abragam and B. Bleaney (Clarendon Press, Oxford 1970).
- 33) T. Moriya, Phys. Rev. **120**, 91 (1960).
- 34) P. M. Richards, M. B. Salamon, Phys. Rev. B **9**, 32 (1974).